biosensors

MDPI

Article

Fabrication of $Co_3O_4/NiCo_2O_4$ Nanocomposite for Detection of H_2O_2 and Dopamine

Tianjiao Liu [1], Xiaoyuan Zhang [1], Kun Fu [1], Nan Zhou [1], Jinping Xiong [2,*] and Zhiqiang Su [1,*]

[1] Beijing Key Laboratory of Advanced Functional Polymer Composites, State Key Laboratory of Chemical Resource Engineering, Beijing University of Chemical Technology, Beijing 100029, China; 2019400133@mail.buct.edu.cn (T.L.); 2020700036@mail.buct.edu.cn (X.Z.); 18811355265@163.com (K.F.); 2021210251@mail.buct.edu.cn (N.Z.)

[2] Beijing Key Laboratory of Electrochemical Process and Technology of Materials, Beijing University of Chemical Technology, Beijing 100029, China

* Correspondence: xiongjp@mail.buct.edu.cn (J.X.); suzq@mail.buct.edu.cn (Z.S.)

Abstract: Herein, the $Co_3O_4/NiCo_2O_4$ nanocomposite has been prepared as a novel electrochemical sensor to accurately detect hydrogen peroxide (H_2O_2) and glucose. ZIF-67 is a metal-organic framework (MOF) with Co as the center metal ion. Co_3O_4 can be obtained by calcination of ZIF-67 at 700 °C, which can retain the structure of ZIF-67. The hollow Co_3O_4 nanocrystal was synthesized based on a calcination process of ZIF-67. This open structure can promote the whole $Co_3O_4/NiCo_2O_4$ nanocomposite larger accessible surface area and reactive sites. Co_3O_4 has good electrocatalytic performance, which has been applied in many fields. Moreover, H_2O_2 and dopamine sensing tests indicate that the as-prepared non-enzymatic electrochemical biosensor has good detection properties. The testing results indicate the as-prepared biosensor has a wide detection range, low detection limit, high selectivity, and long-term stability. These testing results suggest the potential application in food security, biomedicine, environmental detection, and pharmaceutical analysis.

Keywords: ZIF-67; Co_3O_4; $NiCo_2O_4$; electrochemical biosensor; H_2O_2; dopamine

Citation: Liu, T.; Zhang, X.; Fu, K.; Zhou, N.; Xiong, J.; Su, Z. Fabrication of $Co_3O_4/NiCo_2O_4$ Nanocomposite for Detection of H_2O_2 and Dopamine. *Biosensors* **2021**, *11*, 452. https://doi.org/10.3390/bios11110452

Received: 19 October 2021
Accepted: 11 November 2021
Published: 13 November 2021

1. Introduction

Many biomolecules play an essential role in vital activities and biochemical reactions in the human body, such as transmitting biological molecules and responses in natural metabolism [1]. Common biological molecules are glucose [2], uric acid [3], RNA [4], ascorbic acid, hydrogen peroxide (H_2O_2) [5], and dopamine [6,7]. The existence of these substances can maintain the normal physiological activities of the human body. However, once the concentration of these substances is too low or too high, it may cause various diseases. For example, dopamine, produced by the brain, is a typical small biological molecule in the human body to control the emotion of humans. Once the concentration is too high, people may get schizophrenia. On the contrary, if dopamine concentration in the human body is too low, people may get depression [6,7]. H_2O_2 concentration in some parts of the human body is also an important healthy index, which if sustained in a normal range, can keep human health [5,8,9]; therefore, it is very important to detect biological small molecules rapidly and accurately for disease diagnosis and clinic treatment [10,11]. The current methods for detecting these small biological molecules in vivo include fluorescence spectrometry, colorimetric analysis, high-performance liquid chromatography, and electrochemical analysis [12,13].

The electrochemical analysis is usually to establish an electrochemical system. The detected small biological molecules are used as a part of this system, and then the relationship between the current of the system and the concentration of the detected substances is analyzed. This method is named the electrochemical biosensor. Compared to other methods, electrochemical biosensors have low cost, a small volume, an easy to build system, good selectivity, high sensitivity, a fast response, good biocompatibility, and many

other advantages that have attracted the attention of every corner of the world [14–16]. Recent research has reported 3D porous reduced graphene oxide (RGO) decorated with MoS_2 quantum dots to detect H_2O_2. RGO can be used as an electrochemical biosensor to accelerate the ion transform of the reaction system, to improve the electrical property [17]. Another researcher displayed a CuO/PANI hollow nanofiber to detect H_2O_2 and glucose simultaneously. This hollow fiber can provide a more specific surface area, offering more active reaction sites to electrochemical reactions [18]. In addition, there are many other materials used in electrochemical biosensors, which will not be described in this paper.

Metal-organic framework (MOF) is a novel material developed in recent years [19,20]. It forms intramolecular pores by self-assembling organic ligands and metal ions or clusters through coordination bonds. When changing the carbon chain length, the structures and pore sizes can be adjusted [21], and different center metal ions can be introduced to MOF materials with various structures due to other self-assembly methods of different metal ions. Similarly, different functional groups and ligands can also lead to MOF materials with different properties [22–25]. MOF has adjustable pores, an ordered crystal structure, and large specific surface areas widely used in electrocatalysis, gas adsorption, energy storage, and electrochemical sensing [26].

MOF materials can be synthesized by solution, ultrasonic, microwave, diffusion, and hot solvent methods [26]. Among these methods, the solution method is the most common method for synthesizing MOF, a simple stirring process that can produce many MOF materials. This preparation method is also used in this paper. MOF synthesized by the water thermal method generally has two valences of metal ions in these MOF materials. Therefore, the water thermal method mainly focuses on obtaining homogeneous MOF crystals.

ZIF-67 is a kind of hollow polyhedral material and expresses high thermal stability and chemical robustness. Although this structure allows MOF to have a suitable electrochemical property, the conductive property of MOF is not as good. MOF materials are often used in combination with other materials; the doped materials can possess the properties of both materials. The properties of these materials have been improved in all aspects. $NiCo_2O_4$ is a layered double oxide material with a spinel structure. Generally, $NiCo_2O_4$ is synthesized by a simple water-thermal method. The morphology of $NiCo_2O_4$ can be control through different reaction conditions. $NiCo_2O_4$ has many advantages for electrode material, such as cheap, environment-friendly, good electrical conductivity, and abundant REDOX site on the surface. These properties can lead $NiCo_2O_4$ to be more used in modified composite materials to obtain novel materials with improved materials.

In this paper, we proposed a novel $Co_3O_4/NiCo_2O_4$ composite. Hollow Co_3O_4 nanocrystal was obtained by ZIF-67 calcinating at high temperature, and the production had retained the regular dodecahedron structure ZIF-67 possesses. The as-prepared Co_3O_4 has excellent electrochemical properties in electrocatalysis, rechargeable batteries, and electrochemical biosensors. $NiCo_2O_4$ was formed in the nanorod structure, connecting the scattered Co_3O_4 nanocubes to generate Co_3O_4/ $NiCo_2O_4$ composite, which improved electrical property. The as-synthesized material was utilized as the electrochemical biosensors expressed a low detection limit and wide detected range compared to similar biosensors. These properties of as-prepared Co_3O_4/ $NiCo_2O_4$ composite mainly have two advantages in sensing. At first aspect, Co_3O_4/ $NiCo_2O_4$ composite has high specific surface area, which can provide more reaction active sites to electrochemical reaction. On the other hand, Co_3O_4/ $NiCo_2O_4$ composite contain the elements favorable for electrochemical biosensor. When the as-prepared biosensor was used to detect other biomolecules, such as glucose, urea acid, and KCl, the curve had almost no response, which demonstrated that the as-prepared biosensor had good selectivity to H_2O_2 and dopamine. The synthesized process and detection mechanism are provided in Figure 1.

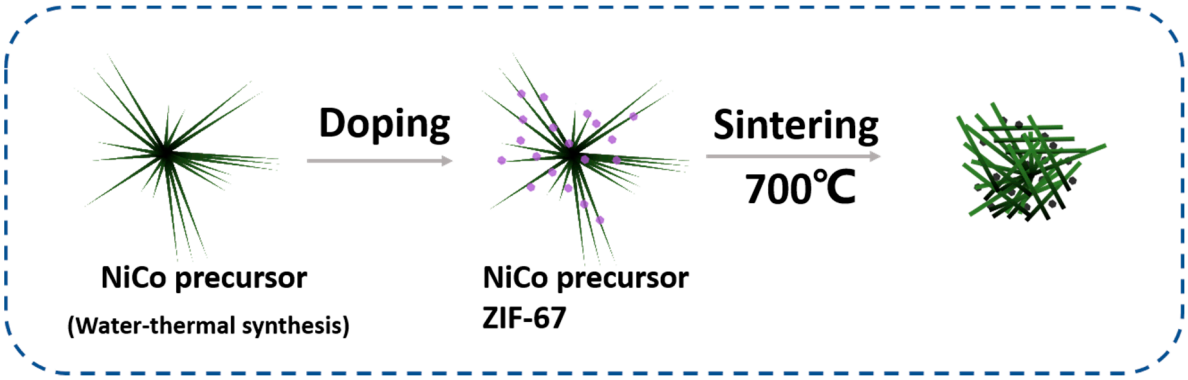

Figure 1. Schematic description for synthesizing $Co_3O_4/NiCo_2O_4$ with high-temperature calcination of the ZIF-67/Ni-Co composite.

2. Materials and Methods

2.1. Materials

Cobalt nitrate hexahydrate ($Co(NO_3)_2 \cdot 6H_2O$), cetyl trimethyl ammonium bromide (CTAB, 99%), phosphate balances normal saline (PBS 1M pH = 7.2–7.4), dopamine (DA, 98%), potassium chloride (KCl, 99.5%), uric acid (UA, 98%) and urea (99%) were purchased from J&K (Beijing, China). Hydrogen peroxide (H_2O_2, 30%) was purchased from Beijing Chemical Co. Ltd. (Beijing, China), glucose was purchased from Macklin Biochemical Co. Ltd. (Shanghai, China). Cobalt chloride ($CoCl_2$, 98%) and nickel chloride ($NiCl_2$, 98%) were purchased from Energy Chemical Co., Ltd. (Shanghai, China). 2-methylimidazole and Nafion (5%) were purchased from Sigma-Aldrich (Shanghai, China). Methanol was purchased from Fuchen Chemical Co., Ltd. The water was purified through a Millipore system (≈18.2 MΩ cm, Zhongyang Technology Development Co., Ltd., Beijing, China).

2.2. Synthesis of Ni-Co Precursor

The Ni-Co precursor was synthesized by a hydrothermal synthesis method. At first, $CoCl_2$ (0.1 mol), $NiCl_2$ (0.05 mol), CTAB (0.04 mol), and urea (0.18 mol) were mixed in moderate deionized (DI) water and stirring for 30 min until all substances were fully dissolved and evenly mixed. Then, the as-prepared light red transparent solution was put in a Teflon-lined container and heated at 100 °C for 12 h. When the reaction finished, the container was taken out after cooling. Next, we centrifuged the reaction solution, collected the precipitation, and washed it three times with DI water and ethyl alcohol. Lastly, the residue was dried in a vacuum oven overnight.

2.3. Synthesis of $Co_3O_4/NiCo_2O_4$

To synthesize $Co_3O_4/NiCo_2O_4$, we synthesized ZIF-67/Ni-Co composite firstly. The as-prepared Ni-Co precursor was immersed in a $Co(NO_3)_2$ (1 mmol) methanol solution, while the Ni-Co precursor concentration in methanol solution was 1 mmol. 4 mmol 2-methylimidazole was put in a 250 mL beaker, we added methanol, and poured the 2-methylimidazole methanol solution into the former solution after 2-methylimidazole was fully dissolved in methanol. The mixed solution was stirring for 30 min and centrifugated after being aged for 24 h.

2.4. Preparation of Electrochemical Biosensor and Electrochemical Test

A three electrodes system synthesized the electrochemical biosensor. In this electrochemical system, a saturated amalgam electrode was used as a reference electrode, a platinum foil electrode was utilized as an auxiliary electrode, and a working electrode was a self-made electrode. Before synthesizing the working electrode, the glass carbon electrode (GCE) had to be polished using 3.0 μm, 0.1 μm, and 0.05 μm alumina polishing powder for 10 min and washed by ethanol dried in the air, respectively. This three-electrode system performed electrochemical tests. The cyclic voltammetry (CV) curve and I-t curve were

measured with a CHI760E electrochemical workstation (Shanghai, China). A PBS solution (0.1 M pH = 7.2–7.4) was used as the electrolyte in all electrochemical tests. Before the electrochemical tests, the PBS solution was fully deoxygenated by nitrogen. All of the tests were carried out under atmospheric conditions, at room temperature.

3. Results and Discussion

3.1. Characterization of $Co_3O_4/NiCo_2O_4$

In this part, some analysis and test methods were used to characterize $Co_3O_4/NiCo_2O_4$ and a series of intermedia products, during the whole preparation process. A scanning electron microscope (SEM, JEOL, S4700, Beijing, China) was used to observe the surface morphology of materials. ZIF-67 crystal was synthesized by the solution precipitation method, as exhibited in Figure 2a; the size scale was around 200–300 nm. The size of ZIF-67 was generally uniform, and the ZIF-67 crystals had a dodecahedron appearance. It was purple to the naked eye. The following intermedia product was Ni-Co nanorods, the precursor material of the $NiCo_2O_4$ nanorod. The morphology of the Ni-Co nanorod is displayed in Figure 2b. Ni-Co precursor was mainly displayed as nanorod morphology, and the diameter of these rods was around 50–100 nm. Moreover, the Ni-Co nanorod was immersed in $Co(NO_3)_2$ methanol solution to absorb Co^{2+}; 2-methylimidazole was added in the former solution to synthesize ZIF-67 on the surface of Ni-Co nanorod. The morphology of ZIF-67/Ni-Co nanocomposite is displayed in Figure 2c–f demonstrate that the morphology of $Co_3O_4/NiCo_2O_4$ is a nanocomposite. The morphology of production did not change much compared to the reactants. After calcination at 700 °C, the previously slippery surface of ZIF-67 contracted and formed many folds.

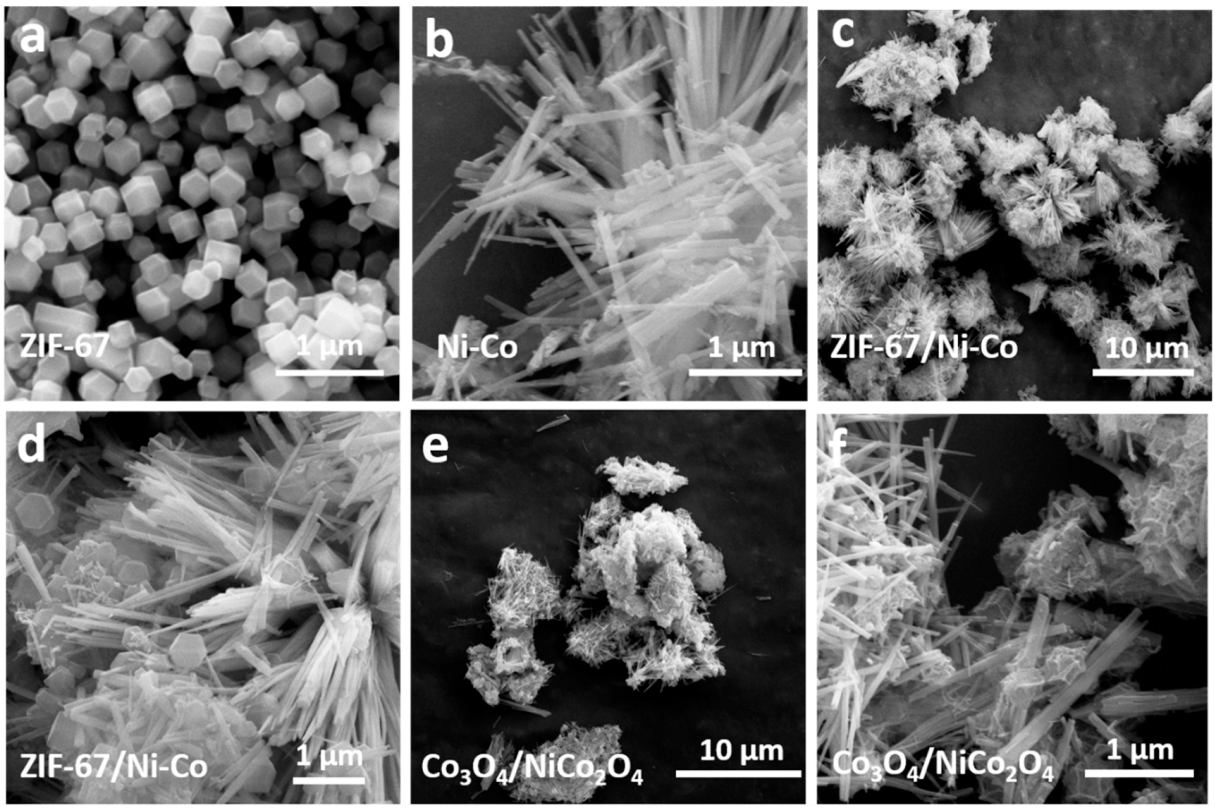

Figure 2. SEM images of the (**a**) ZIF-67 nanocrystal, (**b**) Ni-Co nanorod precursor, (**c**,**d**) ZIF-67/Ni-Co nanocomposite, and (**e**,**f**) $Co_3O_4/NiCo_2O_4$ nanocomposite, in different magnifications.

X-ray diffraction (XRD, Bruker, Ultima IV X) spectrum and X-ray photoelectron spectroscopy (XPS, EDAX, UX-2500MA) were used to characterize productions that occurred during the preparation process, and the test results are displayed in Figure 3. Figure 3a

displays the XRD spectrum of Co_3O_4, $NiCo_2O_4$, and $Co_3O_4/NiCo_2O_4$. The peaks that occurred in Figure 3a conformed to the standard PDF card of $NiCo_2O_4$ (PDF#20-0781) and Co_3O_4 (PDF#42-1467). This indicated that the products could be confirmed to be Co_3O_4, $NiCo_2O_4$, and $Co_3O_4/NiCo_2O_4$. Figure 3b displayed the XPS image of Co_3O_4, $NiCo_2O_4$, and $Co_3O_4/NiCo_2O_4$, and Figure 3c,d displayed the XPS images of Ni 2p and Co 2p, respectively. The XPS images demonstrated the elements found and the surface chemical condition of substances. A C 1s, peak at 284.28 eV, was used to calibrate all peaks in this article. There were two 2p spin orbits of Ni^{2+} and Ni^{3+} in Figure 3c. The fitting peak 872.7 eV represented Ni $2p_{1/2}$, which can be divided into 872.7 eV and 870.8 eV, with a satellite shake-up peak of 879.2 eV. These two peaks represented Ni^{3+} and Ni^{2+}, respectively [27]. Similarly, there were fitting peaks at 855.3 eV (Ni^{3+}) and 853.6 eV (Ni^{2+}) and a satellite shake-up peak of 860.8 eV. These peaks can be found both on $Co_3O_4/NiCo_2O_4$ and $NiCo_2O_4$ curves, which can prove the existence of these two substances. The analysis of Co was the same as Ni in Figure 3d. There were two 2p spin orbits of Co^{2+} and Co^{3+}, and the fitting peaks were at 794.9 eV and 784.5 eV, which were Co $2p_{1/2}$ and Co $2p_{3/2}$. There were also two satellite shake-up peaks at 804.1 eV and 788.6 eV, respectively [28].

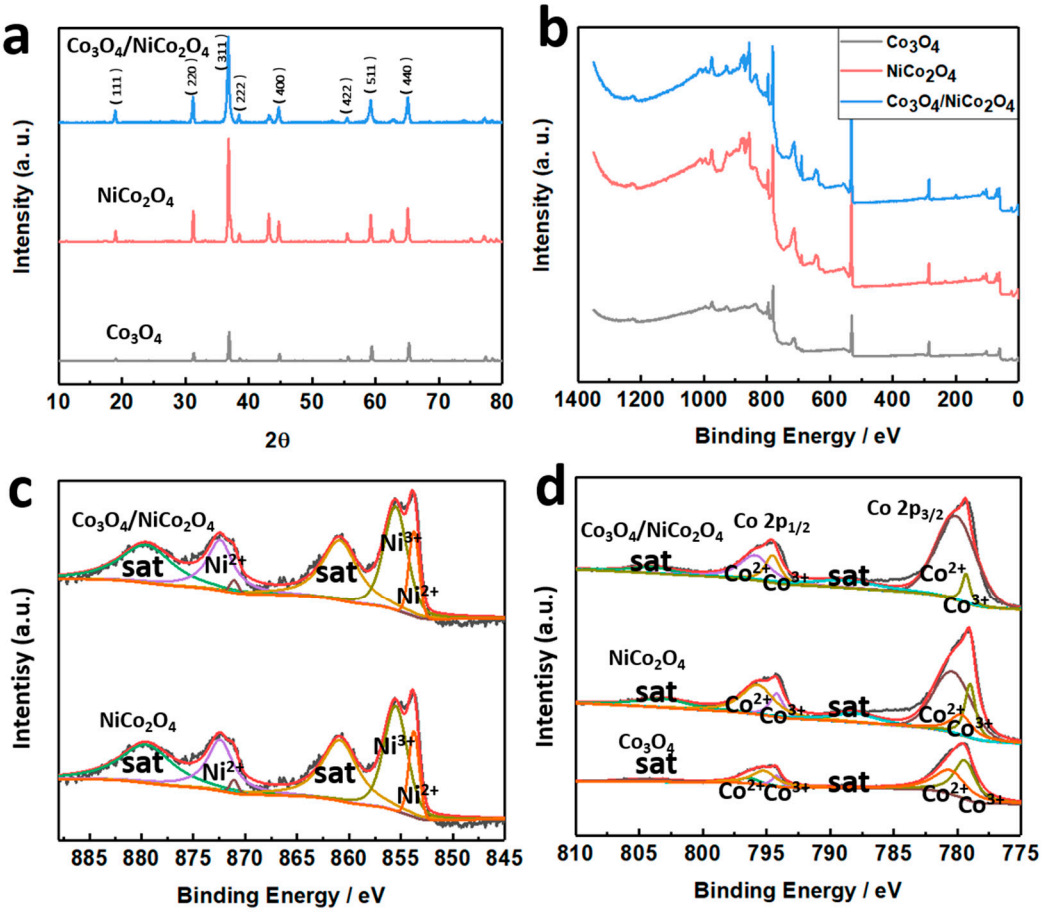

Figure 3. (**a**) XRD spectrum of Co_3O_4, $NiCo_2O_4$, and $Co_3O_4/NiCo_2O_4$, (**b**) XPS of Co_3O_4, $NiCo_2O_4$, and $Co_3O_4/NiCo_2O_4$, (**c**) the result of Ni 2p, and (**d**) Co 2p.

3.2. Electrochemical Tests

The as-prepared materials were used to fabricate electrochemical biosensors to detect hydrogen peroxide (H_2O_2) and dopamine. A three-electrode system established the biosensor. In this system, the self-made $Co_3O_4/NiCo_2O_4$ electrode was used as a working electrode. The method of fabricating a working electrode was introduced in Section 2.4. When the three electrodes system was set up, we first used it to test the CV curve. The potential range was set as −1 to 1 V, and the scanning rate was 50 mV/s. The results of

CVs are displayed in Figure 4. Figure 4a demonstrated the CV curve with H_2O_2 added in different concentrations. The oxidation-reduction peak was enhanced as the concentration of H_2O_2 increased, which demonstrated the effect of H_2O_2 on the electrochemical system. Figure 4b displays the CV curve of Co_3O_4, $NiCo_2O_4$, and $Co_3O_4/NiCo_2O_4$, with the scanning rate at 50 mV/s. Then, the I-t curve was tested based on the three-electrode system; the applied potential was 0.3 V, the sampling interval was 150 s. When H_2O_2 was added to the electrochemical system, the current value suddenly decreased, and the higher the H_2O_2 concentration added, the lower the current was, as displayed in Figure 4c. Figure 4d displays the linear regression curve, drawn with the added concentration and corresponding current. The relationship of added H_2O_2 concentration and corresponding current can be fitted to a line, and the R^2 of this line was equal to 0.98112. The linear regression equation of H_2O_2 detection was $y = -0.01068x - 0.59764$. According to this curve, the limit of detection (LOD) can be calculated as 0.2587 μM (S/N = 3), and the detection range was 0.05–41.7 mM. As an electrochemical biosensor, it must possess as much cyclic time use as possible; Figure 4e,f illustrate the longest cyclic and reuse time of the $Co_3O_4/NiCo_2O_4$ electrochemical biosensor. The CV test of the $Co_3O_4/NiCo_2O_4$ electrode was tested under the condition of adding 50 mM H_2O_2.The results displayed that a self-made $Co_3O_4/NiCo_2O_4$ electrochemical biosensor can retain current at a stable condition for nine days and can be reused at least seven times.

Compared to other similar electrochemical biosensors, the as-prepared self-made $Co_3O_4/NiCo_2O_4$ electrochemical biosensor has advantages. The parameters of various electrochemical biosensors are displayed in Table 1, which indicates that the self-made $Co_3O_4/NiCo_2O_4$ electrochemical biosensor had a wide electrochemical window and low LOD compared with a similar H_2O_2 electrochemical biosensors, which meant that the sensor has high competitiveness in the same sensors.

Table 1. Comparison of the performance of several different H_2O_2 electrochemical sensors.

Materials	Linear Range (mM)	LOD (μM)	Ref.
MnO_2-ERGO paper	0.1–45.4	10	[29]
N-doped hollow carbon sphere (N-HCS)	0.05–47.5	20	[30]
c-ZnO nanosheets	0.001–10	0.8	[31]
Au/Co_3O_4-CeOx nanocomposites	0.01–1	5.29	[32]
Co_3O_4/MWCNTs/gelatin/HRP	0.74–19	0.74	[33]
AgNFs-Pt@BSA/GA/GOD	1–14	300	[34]
v-AuNWs/PDMS	0.04–15	12	[35]
$Co_3O_4/NiCo_2O_4$	0.05–41.7	0.2578	This work

Besides detecting H_2O_2, a self-made $Co_3O_4/NiCo_2O_4$ electrochemical biosensor can also play a role in detecting dopamine. The dopamine electrochemical biosensor experiments were tested by the three-electrode systems mentioned before, and the result of the electrochemical test are displayed in Figure 5. The CV curve of the $Co_3O_4/NiCo_2O_4$ electrochemical biosensor, adding different dopamine concentrations at a scanning rate of 50 mV/s, is displayed in Figure 5a. When the concentration increased, the oxidation-reduction peaks strengthened. The addition of dopamine reacted with active substances in the electrochemical system. Dopamine has two hydroxyl groups in its benzene ring group; when dopamine is added in the electrochemical system, the $Co_3O_4/NiCo_2O_4$ in the electrode oxidize these hydroxyl groups to form quinones, and then quinones are reduced to phenols. Figure 5b displays the CV curves of Co_3O_4, $NiCo_2O_4$, and $Co_3O_4/NiCo_2O_4$ with 50 mM of dopamine, at a scanning rate of 50 mV/s. The I-t curve of $Co_3O_4/NiCo_2O_4$ was used to study dopamine's detection effect, and the result is presented in Figure 5c; the applied potential was 0.3 V and the sampling interval was 150 s. With the adding of dopamine, there was a sudden change in current values. As the concentration increased, the present change increased, which meant a stronger current response. When the I-t test finished, we drew the curve of linear regression curve using current as the Y-axis and adding dopamine

concentration as the X-axis, as demonstrated in Figure 5d with $R^2 = 0.96315$. The linear regression equation of dopamine was $y = -0.00535x - 0.8867$. The detection range of the $Co_3O_4/NiCo_2O_4$ electrochemical dopamine biosensor was 24–329 μM. The LOD was calculated to be 0.2410 μM.

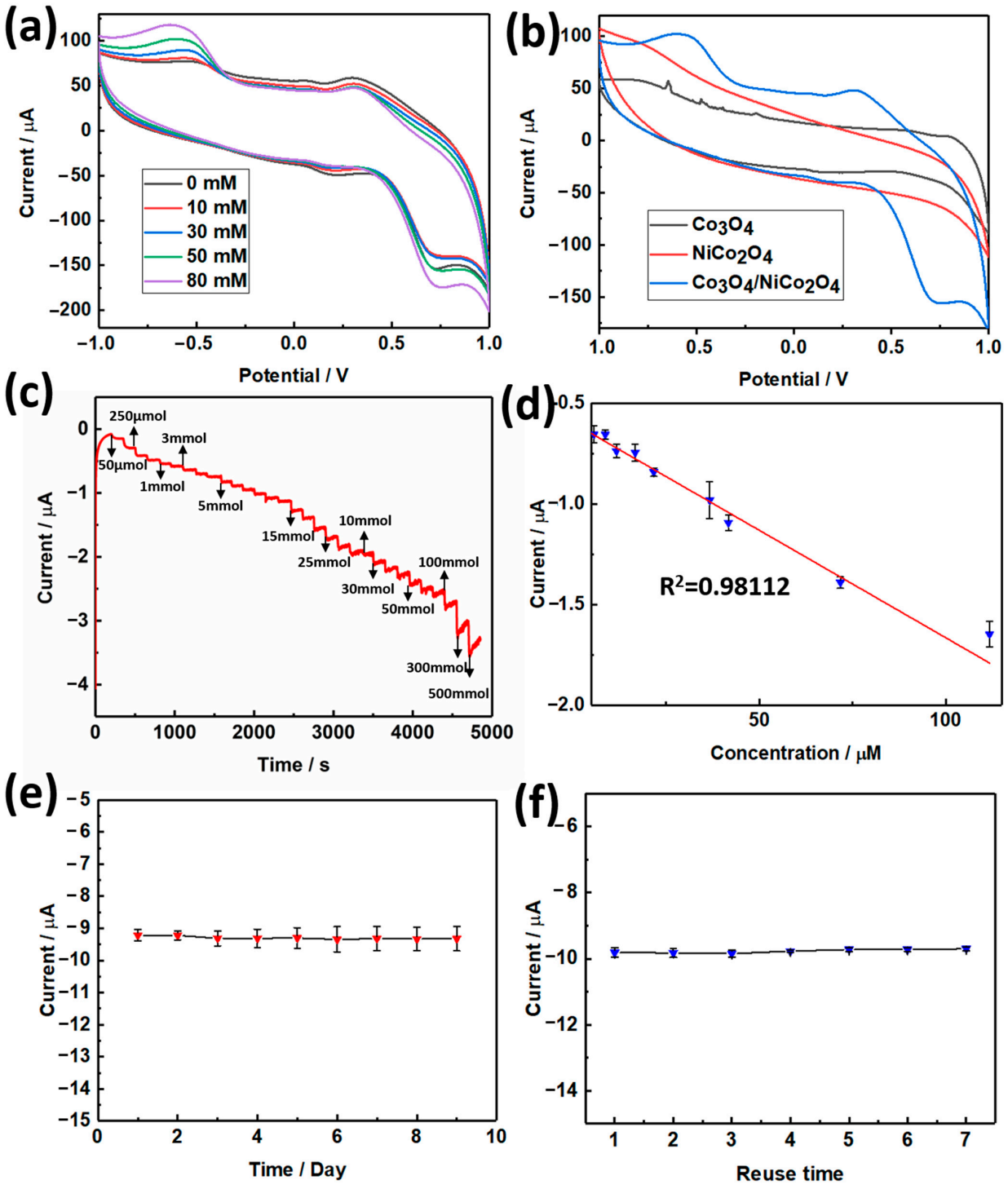

Figure 4. (**a**) The CV of $Co_3O_4/NiCo_2O_4$ at 50 mV/s, adding H_2O_2 in different concentrations. (**b**) The CV of Co_3O_4, $NiCo_2O_4$, and $Co_3O_4/NiCo_2O_4$, with a scanning rate of 50 mV/s. (**c**) The I-t curve of $Co_3O_4/NiCo_2O_4$ when H_2O_2 was added in different concentrations every 150 s. (**d**) The linear regression curve, drawn according to Figure 4c. (**e**) The long time service life test of the H_2O_2 electrochemical biosensor. (**f**) The reuse time test of the H_2O_2 electrochemical biosensor.

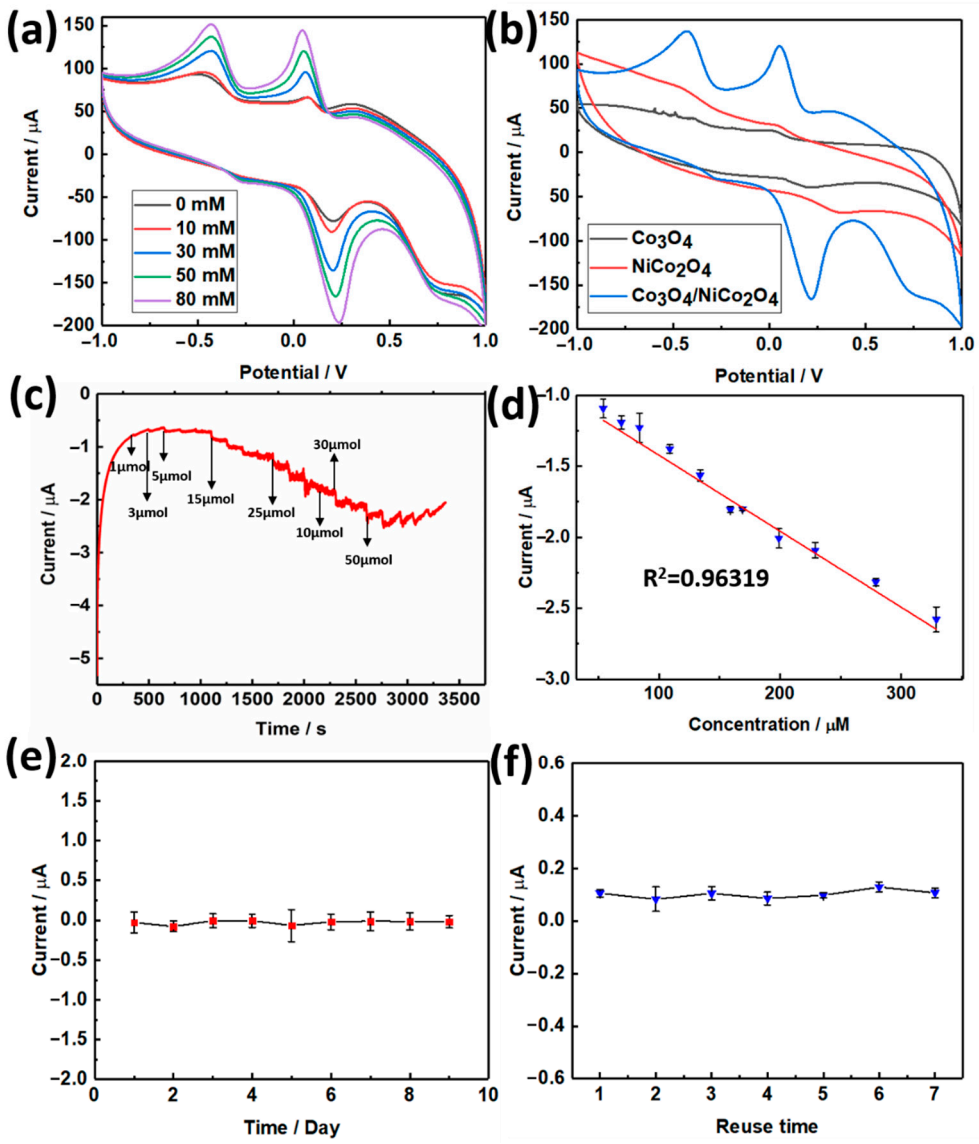

Figure 5. (**a**) The CVs curve of the $Co_3O_4/NiCo_2O_4$ electrochemical biosensor, detecting dopamine with different concentrations at a scanning rate of 50 mV/s. (**b**) The CVs curve of Co_3O_4, $NiCo_2O_4$, $Co_3O_4/NiCo_2O_4$ at a scanning rate of 50 mV/s, with the addition of 50 μM of dopamine. (**c**) The I-t curve of the $Co_3O_4/NiCo_2O_4$ electrochemical biosensor, adding different concentrations of dopamine. (**d**) The linear regression curve, drawn based on Figure 3c. (**e**) The long time service life test of the dopamine electrochemical biosensor. (**f**) Th reuse times test of the dopamine electrochemical biosensor.

Similarly, the long cyclic and reuse time of the electrochemical dopamine biosensor were also tested, as demonstrated in Figure 5d,e. The results in Figure 5e indicate that the electrochemical dopamine biosensor could retain a certain level of initial current value after 15 days, and the dopamine biosensor can be reused eight times, and sustain the initial current, which means the electrochemical dopamine biosensor can be used at least eight times.

Table 2 exhibits several similar electrochemical dopamine biosensors. The as-prepared electrochemical dopamine biosensor was wide in the electrochemical dopamine detection range and low in the detection limitation, compared with similar electrochemical dopamine biosensors. Thus, the as-prepared dopamine electrochemical biosensor had superiority over these similar sensors.

Table 2. Comparison of the performance of several different dopamine electrochemical sensors.

Materials	Linear Range (μM)	LOD (μM)	Ref.
Au-MEA/PEDOT-Tyr	20–300	0.24	[36]
GO/P(ANI-co-THI)	2–500	2	[37]
PA-MNPs/GCE	100–900	7.25	[38]
H-GO/GCE	0.5–40	0.17	[39]
Fe_2O_3–NG/GCE	0.5–10; 10–400	0.08	[40]
IL G	0.679	0.679	[41]
IDEs-SV	0.05–0.25	0.6	[42]
$Co_3O_4/NiCo_2O_4$	24–329	0.2410	This work

The mechanism of the electrochemical biosensor is displayed in Figure 6a. The electrochemical biosensor can react with tested materials and produce an electrical signal proportional to the concentration of tested materials. When H_2O_2 responded with active electrode materials, H_2O_2 would transform to H_2O and O_2. This process would produce a current signal, which was enhanced with increased concentration. The whole reaction process occurred on the surface of the electrode in PBS solution as the electrolyte. Similar to H_2O_2, when dopamine is in contact with the electrode surface, the electrochemical system generates another current signal. The oxidation reaction of catechol to o-quinone in DA occurred, causing the current signal. These processes are exhibited in Figure 6a. Then, to confirm the selectivity of the $Co_3O_4/NiCo_2O_4$ electrochemical biosensor, we chose some small bio-substances, such as glucose, UA, KCl, and AA, as interfering substances with H_2O_2 and dopamine to test the same condition. Figure 6b,c demonstrate that only dopamine and H_2O_2 impact the curve, and other substances have little effect on the curve. This means the self-made electrochemical biosensor has high selectivity to H_2O_2 and dopamine and is undisturbed by other substances.

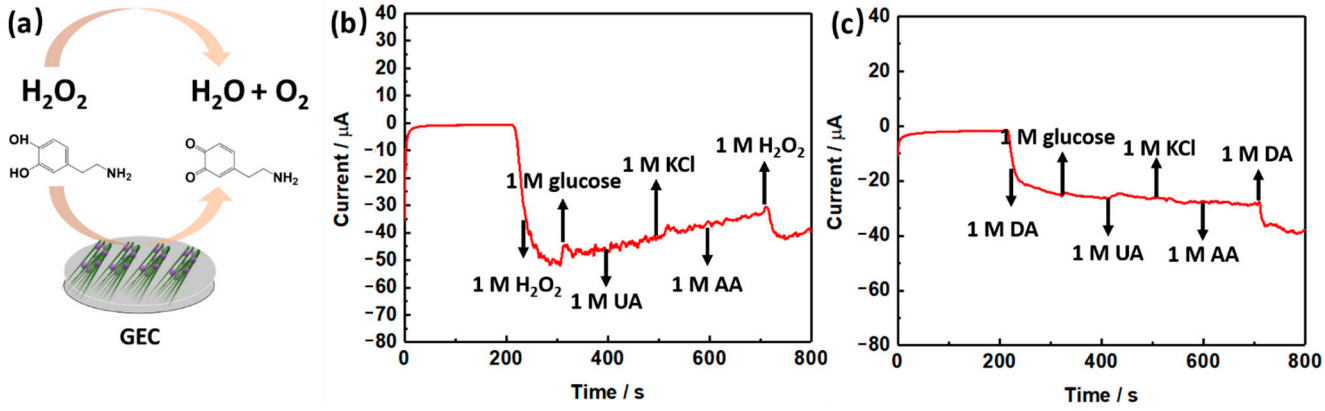

Figure 6. (**a**) The mechanism of electrochemical biosensor detection of H_2O_2 and dopamine. (**b**) The selective ability test of the $Co_3O_4/NiCo_2O_4$ electrochemical biosensor to H_2O_2 and (**c**) DA.

4. Conclusions

In summary, a hollow Co_3O_4 nanocrystal was established based on the $NiCo_2O_4$ nanorod through simple hydrothermal synthesis and a high-temperature calcination method. The $NiCo_2O_4$ nanorod had more free electrons and holes. The structure of the nanorod can reduce polarization. Moreover, the specific surface area of the rod-like structure of $NiCo_2O_4$ was more significant than similar materials. It improved the active sites of a redox reaction, which proved the electrochemical properties of a self-made electrochemical biosensor.

Furthermore, a Co_3O_4 nanocrystal, using ZIF-67 as a matrix, was doped in the $NiCo_2O_4$ nanorod, which also facilitated the properties of the as-prepared nanocomposite. The as-synthesized material next was utilized to fabricate the electrochemical biosensor,

to detect H_2O_2 and dopamine. The $Co_3O_4/NiCo_2O_4$ biosensor can detect H_2O_2 and dopamine simultaneously and has no response with other substances, which illustrates the selectivity of the self-made $Co_3O_4/NiCo_2O_4$ biosensor. More importantly, the self-made $Co_3O_4/NiCo_2O_4$ biosensor had an extensive detection range and low detection limit compared to similar biosensors. When detecting H_2O_2, the detection range was 0.05–41.7 mM, the detection limit was 0.2587 μM, and the detection range of dopamine was 24–329 μM, with the detection limit of 0.2410 μM. These results also indicate that the self-made $Co_3O_4/NiCo_2O_4$ sensors have potential application prospects in future electrocatalysis and electrochemical devices.

Author Contributions: T.L. designed and performed the experiments, analyzed the data, and wrote the paper; Z.S. and J.X. proposed this project and supervised the experiments; X.Z., K.F. and N.Z. conducted final proofreading of the manuscript. All authors have read and agreed to the published version of the manuscript.

Funding: The authors greatly acknowledge the National Natural Science Foundation of China (NSFC, Grant No. 51873016), the Joint Project of BRC-BC (Biomedical Translational Engineering Research Center of BUCT-CJFH) (XK2020-11), and the Fundamental Research Funds for the Central Universities (ZY2103) for their financial support.

Institutional Review Board Statement: Not applicable.

Informed Consent Statement: Not applicable.

Data Availability Statement: Not applicable.

Acknowledgments: Z.S. acknowledges the financial support from the National Natural Science Foundation of China (NSFC, Grant no. 51873016) and the Joint Project of BRC-BC (Biomedical Translational Engineering Research Center of BUCT-CJFH) (XK2020-11). X.Z. acknowledges the financial support from the Fundamental Research Funds for the Central Universities (ZY2103).

Conflicts of Interest: The authors declare no conflict of interest.

References

1. Lopes, I.; Oliveira, A. Human Cytochrome P450 (CYP1A2)-dsDNA Interaction in situ Evaluation Using a dsDNA-electrochemical Biosensor. *Electroanal* **2017**, *29*, 1674–1682. [CrossRef]
2. Yoon, J.; Lee, S.; Shin, M.; Kim, H.; Choi, H.; Lee, T.; Choi, J. Flexible electrochemical glucose biosensor based on GOx/gold/MoS_2/gold nanofilm on the polymer electrode. *Biosens. Bioelectron.* **2019**, *140*, 83–89. [CrossRef] [PubMed]
3. Yang, M.; Wang, H.; Liu, P.; Cheng, J. A 3D electrochemical biosensor based on Super-Aligned Carbon NanoTube array for point-of-care uric acid monitoring. *Biosens. Bioelectron.* **2021**, *179*, 113082. [CrossRef] [PubMed]
4. Li, X.; Li, X.; Li, D.; Zhao, M.; Wu, H.; Shen, B.; Liu, P.; Ding, S. Electrochemical biosensor for ultrasensitive exosomal miRNA analysis by cascade primer exchange reaction and MOF@Pt@MOF nanozyme. *Biosens. Bioelectron.* **2020**, *168*, 112554. [CrossRef]
5. Ma, B.; Li, M.; Cheong, L.; Weng, X.; Shen, C.; Huang, Q. Enzyme-MXene Nanosheets: Fabrication and Application in Electrochemical Detection of H_2O_2. *J. Inorg. Mater.* **2020**, *35*, 131–138.
6. Xie, X.; Wang, D.; Guo, C.; Liu, Y.; Rao, Q.; Lou, F.; Li, Q.; Dong, Y.; Li, Q.; Yang, H.; et al. Single-Atom Ruthenium Biomimetic Enzyme for Simultaneous Electrochemical Detection of Dopamine and Uric Acid. *Anal. Chem.* **2021**, *93*, 4916–4923. [CrossRef]
7. Xiao, L.; Zheng, S.; Yang, K.; Duan, J.; Jiang, J. The construction of CoP nanoparticles coated with carbon layers derived from core-shell bimetallic MOF for electrochemical detection of dopamine. *Microchem. J.* **2021**, *168*, 106432. [CrossRef]
8. Zhu, H.; Tang, W.; Ma, Y.; Wang, Y.; Tan, H.; Li, Y. Preyssler-type polyoxometalate-based crystalline materials for the electrochemical detection of H_2O_2. *Crystengcomm* **2021**, *23*, 2071–2080. [CrossRef]
9. Chang, C.; Chen, Q.; Fan, G. Synergetic enhancement of electrochemical H_2O_2 detection in a nitrogen-doped carbon encapsulated FeCo alloy architecture. *Analyst* **2021**, *146*, 971–978. [CrossRef]
10. Sheng, Z.; Gan, Z.; Huang, H.; Niu, R.; Han, Z.; Jia, R. M-Nx (M = Fe, Co, Ni, Cu) doped graphitic nanocages with High specific surface Area for non-enzymatic electrochemical detection of H_2O_2. *Sens. Actuators B Chem.* **2020**, *305*, 127550. [CrossRef]
11. Zhang, X.; Mao, Z.; Zhao, Y.; Wu, Y.; Liu, C.; Wang, X.F. Highly sensitive electrochemical sensing platform: Carbon cloth enhanced performance of Co_3O_4/rGO nanocomposite for detection of H_2O_2. *J. Mater. Sci.* **2020**, *55*, 5445–5457. [CrossRef]
12. Kumar, S.; Singh, R. Recent optical sensing technologies for the detection of various biomolecules: Review. *Opt. Laser Technol.* **2021**, *134*, 106620. [CrossRef]
13. Hughes, J.; Izake, E.; Lott, W.; Ayoko, G.; Sillence, M. Ultra sensitive label free surface enhanced Raman spectroscopy method for the detection of biomolecules. *Talanta* **2014**, *130*, 20–25. [CrossRef] [PubMed]

14. Farzin, M.; Abdoos, H. A critical review on quantum dots: From synthesis toward applications in electrochemical biosensors for determination of disease-related biomolecules. *Talanta* **2021**, *224*, 121828. [CrossRef]
15. Kim, B.; Lee, H.; Lee, N. A durable, stretchable, and disposable electrochemical biosensor on three-dimensional micro-patterned stretchable substrate. *Sens. Actuators B Chem.* **2019**, *283*, 312–320. [CrossRef]
16. Li, Q.; Wu, J.; Liu, Y.; Qi, X.; Jin, H.; Yang, C.; Liu, J.; Li, G.; He, Q. Recent advances in black phosphorus-based electrochemical sensors: A review. *Anal. Chim. Acta* **2021**, *1170*, 338480. [CrossRef]
17. Lin, D.; Su, Z.; Wei, G. Three-dimensional porous reduced graphene oxide decorated with MoS_2 quantum dots for electrochemical determination of hydrogen peroxide. *Mater. Today Chem.* **2018**, *7*, 76–83. [CrossRef]
18. Liu, T.; Guo, Y.; Zhang, Z.; Miao, Z.; Zhang, X.; Su, Z. Fabrication of hollow CuO/PANI hybrid nanofibers for non-enzymatic electrochemical detection of H_2O_2 and glucose. *Sens. Actuators B Chem.* **2019**, *286*, 370–376. [CrossRef]
19. Ding, M.; Flaig, R.; Jiang, H.; Yaghi, O. Carbon capture and conversion using metal-organic frameworks and MOF-based materials. *Chem. Soc. Rev.* **2019**, *48*, 2783–2828. [CrossRef] [PubMed]
20. Zhao, M.; Huang, Y.; Peng, Y.; Huang, Z.; Ma, Q.; Zhang, H. Two-dimensional metal-organic framework nanosheets: Synthesis and applications. *Chem. Soc. Rev.* **2018**, *47*, 6267–6295. [CrossRef]
21. Farrusseng, D.; Aguado, S.; Pinel, C. Metal-Organic Frameworks: Opportunities for Catalysis. *Angew. Chem. Int. Ed.* **2009**, *48*, 7502–7513. [CrossRef]
22. Vermoortele, F.; Bueken, B.; Le Bars, G.; Van de Voorde, B.; Vandichel, M.; Houthoofd, K.; Vimont, A.; Daturi, M.; Waroquier, M.; Van Speybroeck, V.; et al. Synthesis Modulation as a Tool To Increase the Catalytic Activity of Metal-Organic Frameworks: The Unique Case of UiO-66(Zr). *J. Am. Chem. Soc.* **2013**, *135*, 11465–11468. [CrossRef]
23. Zou, R.; Sakurai, H.; Han, S.; Zhong, R.; Xu, Q. Probing the lewis acid sites and CO catalytic oxidation activity of the porous metal-organic polymer [Cu(5-methylisophthalate)]. *J. Am. Chem. Soc.* **2007**, *129*, 8402–8403. [CrossRef]
24. Horike, S.; Dinca, M.; Tamaki, K.; Long, J. Size-selective lewis acid catalysis in a microporous metal-organic framework with exposed Mn^{2+} coordination sites. *J. Am. Chem. Soc.* **2008**, *130*, 5854–5855. [CrossRef] [PubMed]
25. Hwang, J.; Ejsmont, A.; Freund, R.; Goscianska, J.; Schmidt, B.; Wuttke, S. Controlling the morphology of metal-organic frameworks and porous carbon materials: Metal oxides as primary architecture-directing agents. *Chem. Soc. Rev.* **2020**, *49*, 3348–3422. [CrossRef] [PubMed]
26. Yang, Q.; Xu, Q.; Jiang, H. Metal-organic frameworks meet metal nanoparticles: Synergistic effect for enhanced catalysis. *Chem. Soc. Rev.* **2017**, *46*, 4774–4808. [CrossRef]
27. Fang, Y.; Qi, J.; Wang, F.; Hao, Y.; Zhu, J.; Zhang, P. Highly Durable Passive Direct Methanol Fuel Cell with Three-Dimensional Ordered Porous $NiCo_2O_4$ as Cathode Catalyst. *Chemelectrochem* **2020**, *7*, 2314–2324. [CrossRef]
28. Wang, Y.; Chen, Z.; Fang, R.; Li, Y. Hollow-Co_3O_4@Co_3O_4@SiO_2 Multi-Yolk-Double-Shell Nanoreactors for Highly Efficient CO Oxidation. *Chemcatchem* **2019**, *11*, 772–779. [CrossRef]
29. Jia, W.Z.; Guo, M.; Zheng, Z.; Yu, T.; Rodriguez, E.G.; Wang, Y.; Lei, Y. Electrocatalytic oxidation and reduction of H_2O_2 on vertically aligned Co_3O_4 nanowalls electrode: Toward H_2O_2 detection. *J. Electroanal. Chem.* **2009**, *625*, 27–32. [CrossRef]
30. Peng, C.; Zhou, S.; Zhang, X.; Zeng, T.; Zhang, W.; Li, H.; Liu, X.; Zhao, P. One pot synthesis of nitrogen-doped hollow carbon spheres with improved electrocatalytic properties for sensitive H_2O_2 sensing in human serum. *Sens. Actuators B Chem.* **2018**, *270*, 530–537. [CrossRef]
31. Rui, Q.; Komori, K.; Tian, Y.; Liu, H.; Luo, Y.; Sakai, Y. Electrochemical biosensor for the detection of H_2O_2 from living cancer cells based on ZnO nanosheets. *Anal. Chim. Acta* **2010**, *670*, 57–62. [CrossRef] [PubMed]
32. Liu, H.; Ding, Y.; Yang, B.; Liu, Z.; Liu, Q.; Zhang, X. Colorimetric and ultrasensitive detection of H_2O_2 based on Au/Co_3O_4-CeO_x nanocomposites with enhanced peroxidase-like performance. *Sens. Actuators B Chem.* **2018**, *271*, 336–345. [CrossRef]
33. Kacar, C.; Dalkiran, B.; Erden, P.; Kilic, E. An amperometric hydrogen peroxide biosensor based on Co_3O_4 nanoparticles and multiwalled carbon nanotube modified glassy carbon electrode. *Appl. Surf. Sci.* **2014**, *311*, 139–146. [CrossRef]
34. Huang, Z.; Zhang, A.; Zhang, Q.; Pan, S.; Cui, D. Electrochemical Biosensor Based on Dewdrop-Like Platinum Nanoparticles-Decorated Silver Nanoflowers Nanocomposites for H_2O_2 and Glucose Detection. *J. Electrochem. Soc.* **2019**, *166*, B1138–B1145. [CrossRef]
35. Lyu, Q.; Zhai, Q.; Dyson, J.; Gong, S.; Zhao, Y.; Ling, Y.; Chandrasekaran, R.; Dong, D.; Cheng, W. Real-Time and In-Situ Monitoring of H_2O_2 Release from Living Cells by a Stretchable Electrochemical Biosensor Based on Vertically Aligned Gold Nanowires. *Anal. Chem.* **2019**, *91*, 13521–13527. [CrossRef]
36. Lete, C.; Lakard, B.; Hihn, J.; del Campo, F.; Lupu, S. Use of sinusoidal voltages with fixed frequency in the preparation of tyrosinase based electrochemical biosensors for dopamine electroanalysis. *Sens. Actuators B Chem.* **2017**, *240*, 801–809. [CrossRef]
37. Song, N.; Wang, Y.; Yang, X.; Zong, H.; Chen, Y.; Ma, Z.; Chen, C. A novel electrochemical biosensor for the determination of dopamine and ascorbic acid based on graphene oxide/poly(aniline-co-thionine) nanocomposite. *J. Electroanal. Chem.* **2020**, *873*, 114352. [CrossRef]
38. Chandra, S.; Arora, K.; Bahadur, D. Impedimetric biosensor based on magnetic nanoparticles for electrochemical detection of dopamine. *Mater. Sci. Eng. B Adv.* **2012**, *177*, 1531–1537. [CrossRef]
39. Zou, H.; Li, B.; Luo, H.; Li, N. A novel electrochemical biosensor based on hemin functionalized graphene oxide sheets for simultaneous determination of ascorbic acid, dopamine and uric acid. *Sens. Actuators B. Chem.* **2015**, *207*, 535–541. [CrossRef]

40. Liu, H.; Xiong, R.; Zhong, P.; Li, G.; Liu, J.; Wu, J.; Liu, Y.; He, Q. Nanohybrids of shuttle-like a-Fe_2O_3 nanoparticles and nitrogen-doped graphene for simultaneous voltammetric detection of dopamine and uric acid. *New J. Chem.* **2020**, *44*, 20797. [CrossRef]
41. Wang, C.; Xu, P.; Zhuo, K. Ionic Liquid Functionalized Graphene-Based Electrochemical Biosensor for Simultaneous Determination of Dopamine and Uric Acid in the Presence of Ascorbic Acid. *Electroanalysis* **2014**, *26*, 191–198. [CrossRef]
42. Lupu, S.; Lete, C.; Campo, F. Dopamine Electroanalysis Using ElectrochemicalBiosensors Prepared by aSinusoidal Voltages Method. *Electroanalysis* **2015**, *27*, 1649–1659. [CrossRef]